JGR Biogeosciences

RESEARCH ARTICLE
10.1029/2023JG007575

Key Points:

- Distributions of inorganic Hg^{II} and methylmercury were studied on both sides of the sediment-water interface of the Rhône prodelta
- The epibenthic zone is a place of intense mobilization of inorganic Hg^{II}, whereas methylmercury remains tied to sediments

Supporting Information:

Supporting Information may be found in the online version of this article.

Correspondence to:

D. Cossa,
dcossa@ifremer.fr

Citation:

Cossa, D., Dang, D. H., & Thomas, B. (2024). Mercury mobility in epibenthic waters of a deltaic environment. *Journal of Geophysical Research: Biogeosciences*, *129*, e2023JG007575. https://doi.org/10.1029/2023JG007575

Received 1 JUN 2023
Accepted 2 JAN 2024

Author Contributions:

Conceptualization: Daniel Cossa
Formal analysis: Daniel Cossa, Duc Huy Dang, Bastien Thomas
Investigation: Daniel Cossa, Duc Huy Dang
Methodology: Daniel Cossa, Bastien Thomas
Validation: Daniel Cossa
Writing – original draft: Daniel Cossa
Writing – review & editing: Daniel Cossa, Duc Huy Dang

Mercury Mobility in Epibenthic Waters of a Deltaic Environment

Daniel Cossa[1,2], Duc Huy Dang[3], and Bastien Thomas[2]

[1]Université Grenoble Alpes, Université Savoie Mont Blanc, CNRS, IRD, IFTTAR, Grenoble, France, [2]Ifremer, Centre Atlantique, Nantes, France, [3]School of the Environment and Department of Chemistry, Trent University, Peterborough, ON, Canada

Abstract Mercury (Hg) cycling at the sediment-water interfaces (SWI) encompasses multiple homogeneous and heterogeneous biogeochemical reactions whose result is not yet elucidated. Estuarine SWIs, where the organic matter mineralization is active, constitute experimental sites particularly suitable for scrutinizing Hg speciation and mobilization. Here, we present high-resolution vertical concentration profiles of Hg species, including inorganic divalent Hg (Hg^{II}_{inorg}) and monomethyl Hg (MMHg) in solid and dissolved (<0.22 μm) phases, on both sides of the SWI of the proximal part of the Rhône prodelta (northwestern Mediterranean Sea) using sediment cores and dialyzers implemented for a 67-day-long period. Concentrations of the dissolved Hg^{II}_{inorg} species were <0.10 nM in the sediment pore waters but reached up to 0.58 nM in the epibenthic water zone, a concentration level that is ∼200 times higher than that of the water column. Conversely, MMHg concentrations were low (<0.5 pM) above the SWI and increased to up to 4.6 pM in the sulfate-reducing zones of the sediment. The dynamic of the Hg species interconversions was explored using one-dimensional transport-reaction equations. This model allowed us to constrain the depth intervals where various species are produced or consumed and to approximate the reaction rates. We conclude that the epibenthic zone of the Rhône prodelta is a location of intense mobilization of inorganic Hg^{II} associated with organic matter mineralization and MMHg distribution in pore water is controlled by microbiological in situ reactions, but sedimentary MMHg does not diffuse in the overlying water column.

Plain Language Summary Mercury (Hg), especially its monomethylated form (MMHg) is a harmful metal to marine life. Coastal sediments are an important site for natural and anthropogenic Hg accumulation. However, its sequestration in the sediments may not be permanent since chemical and microbiological processes may mobilize dissolved Hg species on both sides of the sediment-water interface. We show that the proximal zone of the Rhône prodelta is a place of intense mobilization of inorganic Hg in the immediate vicinity above the sediment and that the diffusion of MMHg from sediment pore water is not a major Hg source for the overlying water column. Our results imply that the MMHg produced in the pore waters may reach the water column above sediments, where it can be bioaccumulated in epibenthic organisms and biomagnified in their related food webs, but mainly in conjunction with sediment resuspension.

1. Introduction

Mercury (Hg) and its compounds are harmful to the environment and their availability for marine life is a major issue (e.g., Boening, 2000; Mergler, 2021). In addition to being highly toxic, monomethylHg (MMHg) is the most available form of Hg for phytoplankton (e.g., Gosnell & Mason, 2015; Lee & Fisher, 2017). Moreover, it is the chemical species that biomagnifies along aquatic food webs (e.g., Lavoie et al., 2013; Tesán-Onrubia et al., 2023). The inorganic divalent Hg forms (Hg^{II}_{inorg}), which include numerous charged and neutral complexes (Gworek et al., 2016), constitute a significant group of species since some of them are substrates for Hg methylation when biogeochemical conditions become favorable (e.g., Fitzgerald et al., 2007; Mason et al., 2012). A major outcome of the research concerning the Hg biomagnification in marine food webs is that, regardless of the chemical species, the highest Hg bioconcentration factor occurs between water and primary producers (10^3–10^5) (AMAP/UN Environment, 2019; Lee & Fisher, 2017; Mason et al., 1996). It is, thus, crucial, for assessing the ecosystems' exposure to Hg, to explore in a first step the bioavailability of Hg for autotrophic microorganisms, that is, to explore the Hg speciation of dissolved Hg in waters. In coastal waters, dissolved Hg originates from the atmosphere, continental runoff, marine waters, and sediments. Several studies suggested that, in Hg-contaminated coastal environments, the sediments can be a significant source of dissolved Hg^{II}_{inorg} and

MMHg for the overlying waters (Bothner et al., 1980; Covelli et al., 1999; Gill et al., 1999; Gobeil & Cossa, 1993; Merritt & Amirbahman, 2008; Muresan et al., 2007; Rigaud et al., 2013). It was also argued that, in most coastal marine environments including estuaries, the sediment would be a major MMHg source for ecosystems (e.g., Hammerschmidt et al., 2004; Hollweg et al., 2010). Hammerschmidt & Fitzgerald (2006) even asserted that the diffusive flux of MMHg from the shelf sediments is sufficient to sustain the rate of MMHg accumulation by marine fish in Long Island Sound. At a global scale, based on Hg concentrations in tuna and a model of the Hg cycle, Kraepiel et al. (2003) have suggested that oceanic MMHg should be formed in deep waters or sediments. On the other hand, mass budget calculations in Bay of Fundy sediments have revealed that MMHg fluxes into sediments from settling solids exceed losses from sediment-to-water diffusion and resuspension, which suggests that inflowing fluvial and tidal waters, rather than coastal sediments, are the dominant MMHg sources for pelagic marine food webs (Sunderland et al., 2010). The latter conclusion is supported by a study of several estuaries that fail to observe any correlation between the water column MMHg and the sediment Hg, suggesting that additional sources of MMHg should regulate water column MMHg levels (Balcom et al., 2015). These conflicting results may be explained by the various Hg biogeochemical transformations during the early diagenesis of the organic matter (OM). Early studies (e.g., Bothner et al., 1980) and more recent (e.g., Frieling et al., 2023) have suggested that redox conditions influence Hg speciation and Hg flux across the sediment-water interface (SWI). Indeed, the redox conditions, determined by the dynamic of OM degradation, control the Hg solubilization through phase and speciation changes (e.g., Chakraborty et al., 2015; Oliveri et al., 2016; Sunderland & Mason, 2007), and may favor the MMHg abundance depending on the type of OM degradation and the type of associated bacteria (e.g., Bravo & Cosio, 2019; Cossa et al., 2014; Merritt & Amirbahman, 2009). Coastal sediments house more than 80% of the globally buried OM in the oceans (Berner, 1989). Furthermore, near-shore estuarine sediments, including deltaic zones, are organic-rich from both terrestrial and marine sources loaded with microorganisms (Aller & Aller, 2004) and, thus, constitute sites of intense mineralization of OM via oxic, sub-oxic, and anoxic pathways (e.g., Berner, 1980; Burdige, 2005). The early diagenesis of OM comes with Hg transformations (Hong et al., 2014; Marvin-DiPasquale & Agee, 2003; Sanei et al., 2012), thus, estuarine and deltaic sediments turn out to be among the most suitable environments for gaining further understanding of Hg dynamics and sources for coastal ecosystems. Despite this situation, the biogeochemical transformations undergone by Hg in coastal sediment are yet poorly understood and there is still large uncertainty about the importance of coastal sediments as a source of Hg species for the overlying water column. In other words, the post-depositional mobility of Hg in coastal sediment, and its possible efflux to the water column, remains a crucial and controversial issue.

Most of the published studies concluding there is a flux of MMHg across the sediment-water interface have been based on low-resolution modeling, and there has been a general shortage of related empirical measurements in the epibenthic zone. In order to address the associated knowledge gaps, we here present high-resolution profiles of dissolved Hg^{II}_{inorg}, MMHg, and redox tracers on both sides (from the epibenthic zone to pore waters) of the SWI of the Rhône prodelta sediments. The dynamic of the Hg species interconversions was explored using one-dimensional transport-reaction equations. This model allowed us to constrain the depth intervals where various species are produced or consumed and to approximate the reaction rates. This paper examines how the particular biogeochemical context of organic-rich marine sediments, like those of the Rhône prodelta, influences the dynamics of Hg speciation, partition, and mobility.

2. The Rhône Pro-Delta Settings

The Rhône River (RR), with a catchment area of approximately 10^5 km^2 and average water discharge and suspended solids loading of 1,700 m^3 s^{-1} and 3 Mt a^{-1}, respectively (Antonelli, 2002; Pont et al., 2002;), is the first river in the Mediterranean basin in terms of flows since the construction of the Aswan Dam on the Nile. The Rhône watershed accounts for more than 90% of the terrigenous solid contributions to the Gulf of Lion (GoL) (Gangloff et al., 2017). About 80% of the suspended particulate material delivered by the RR accumulates in its prodelta, mainly as pulsed events during flooding periods (e.g., Miralles et al., 2005; Roussiez et al., 2006; Ulses et al., 2008). This particulate material is organic-rich (2%–3%) and loads approximately 0.2 Mt of carbon annually (Sempéré et al., 2000). As a result of the abrupt fall of turbulence, massive sedimentation rates (SR) occur at the mouth of the RR (30–50 cm a^{-1}), especially during flood events (Cathalot et al., 2010; Charmasson et al., 1998; Marion et al., 2010; Wu et al., 2018; Zebracki et al., 2015), and contribute in the construction of the sedimentary prism. From the numerous studies assessing the benthic OM mineralization (e.g.,Cathalot, 2008; Cathalot et al., 2010; Lansard et al., 2009; Pastor et al., 2011a, 2018; Tesi et al., 2007), the main characteristics of

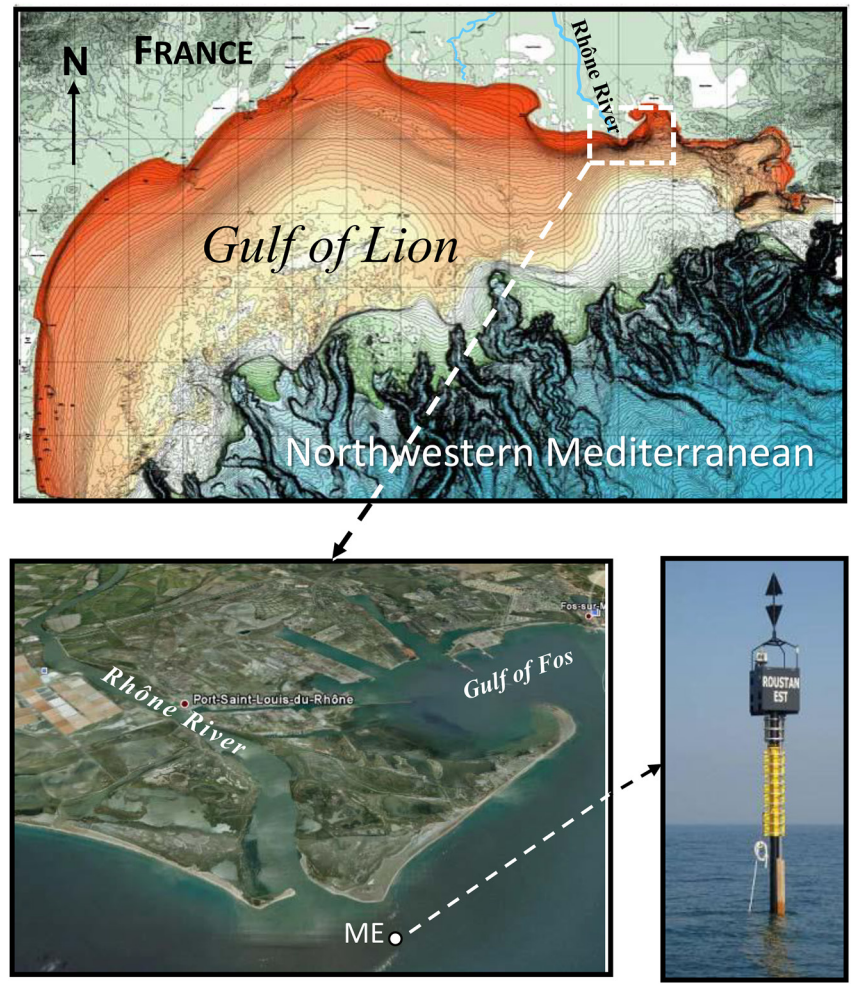

Figure 1. Sampling location in the Rhône prodelta.

the prodelta can be summarized: (a) a large amount of sedimentary OM is buried (60%) on-site, (b) the terrestrial OM inputs govern a degradation mainly driven by sulfate reduction, and (c) most of the major reduced species are sequestered and their diffusion to the oxic zone is limited.

3. Material and Methods

3.1. Sampling

The experimental site was located in the proximal part of the Rhône prodelta (the Roustan lobe) at the MESUHRO buoy (Sta. ME, 43°19.2′ N, 4°52.0′ E, Figure 1), located less than 2.5 km from the RR mouth, by 20 m depth. Sampling operations were carried out by divers. Two ~30 cm-long sediment cores (ME-1 and ME-2) were collected on 5 May 2011, using a 6 cm diameter Teflon jar open at both ends (PFA 2L jar, Savillex). After collection, the cores were maintained at +10°C until subsampling in the laboratory, where they were sliced at every centimeter from SWI down to 8 cm, then at every 3 cm to the bottom of the core, for a total of 15 levels. The resulting samples were frozen, freeze-dried, and stored in the dark at +4°C until analyzed. Four dialyzers, called Peepers A, B, C, and D (Figure S1 in Supporting Information S1), were inserted in sediments for 67 days (May 5–11 July 2011) to collect pore-waters. Initially conceived by Hesslein (1976), and then designed by numerous authors (e.g., Adams, 1994; Carignan et al., 1985), the Peepers' technique has been validated for studying Hg and MMHg in sediments (Mason et al., 1998). Here, we used methacrylate Peepers with a 0.22 µm porosity polycarbonate membrane, consisting of 50 dialysis cells spaced 1.0 cm apart. They were conditioned under nitrogen 15 days before launching to keep them under anoxia. After capping, the Peepers were transported in a special case

and kept under nitrogen until they were processed in the laboratory (Figure S2 in Supporting Information S1). Transport and laboratory treatment times were less than 4 hr. Eight (8) mL of pore water were collected at each of the 50 levels of the four Peepers A, B, C, and D. Sub-samples were collected in Teflon tubes (PFAs) for Hg speciation, and in polypropylene or borosilicate glass for other chemical species. The tubes for Hg speciation were washed with 10% HCl (v:v) and then rinsed with Milli-Q water before utilization. The sub-samples were kept acidified (HCl Suprapur, Merck at 0.8% v:v), at +4°C in the dark. The four Peeper's cell contents were analyzed for Hg speciation using the Geotraces ultra-trace protocols (Bowie & Lohan, 2008), whereas, because of the limited volume of pore water, only those from Peepers B and C were analyzed for redox-sensitive elements.

3.2. Analyses

Concentrations of Hg^{II}_{inorg} and MMHg in pore waters were simultaneously determined using a method based on hydriding and gas chromatography coupled (GC) with atomic fluorescence spectroscopy (AFS) detection, according to a protocol developed by Stoichev et al. (2004) and further modified by Cossa et al. (2009). In brief, the volatile compounds formed by hydruration are concentrated by a cryogenic procedure on a column filled with Chromosorb W/AW-DMCS (60/80 mesh impregnated with 15% OV-3) in a liquid nitrogen bath before being progressively released by heating the column to 90°C. The compounds are thermally decomposed into Hg^0 within a furnace (800°C) and then transported by an argon current to the AFS (Mercury analyzer model 2500, Tekran). The method's reproducibility varies from 6% to 15% depending on the species and the concentration in the sample analyzed. For an aliquot of 10 mL, the detection limits were 0.06 and 10 pM for MMHg and Hg^{II}_{inorg}, respectively.

Solid-phase total Hg was determined by atomic absorption spectrophotometry after dry mineralization and pre-concentration on a gold trap using a semi-automatic instrument (Model AMA-254, Altec). The method detection limit was 7 ng g^{-1}. The reproducibility was 2% ($n = 6$). Accuracy was checked using MESS-2 (National Research Council of Canada) as a certified reference material (CRM), and the values obtained (92 ± 2 ng g^{-1}) were always within the range of the certified values (92 ± 9 ng g^{-1}). MMHg in solid samples was determined by propylation with gas chromatography-inductively coupled plasma mass spectrometry coupling (GC-ICP-MS) according to the procedure described by Abi-Ghanem et al. (2011). Quantification was performed by isotopic dilution using an ICP-MS (GC-Focus with X-series, Thermo Electron). In brief, a known quantity of $MM^{202}Hg$ was added to the sediments, and MMHg was extracted using HNO_3 and propylated using sodium tetrapropylborate solution. The propyl-methylHg was extracted into iso-octane, which was injected into the GC-ICP-MS coupling. The detection limit for the MMHg method was 0.02–1.00 ng g^{-1} and the precision was 20%–30% depending on the concentration. The accuracy was established using CRM IAEA-405 from the International Atomic Energy Agency. The average concentration obtained for IAEA-405 was 5.49 ± 0.4 ng g^{-1} compared to the certified value of 5.49 ± 0.3 ng g^{-1}.

Determinations of dissolved Si, Na, Mg, K, Ca, P, Fe, and Mn were performed by atomic emission spectrometry-inductively coupled plasma coupling (ICP-AES). Sulfate was analyzed using a spectrometric technique, as previously described by Dang et al. (2014a), by which BaCl2 was added to HNO3-acidified seawater samples to induce barium sulfate precipitation. The latter was kept suspended in solution by a detergent (Tween20, Sigma-Aldrich) and measured at 660 nm using spectrophotometry (DR-2800, Hach Lange). Organic carbon (C_{org}) was determined using freeze-dried and homogenized subsamples of sediments with an elemental analyzer (Model CN-2000, LECO) after acidification with 2 M HCl (overnight, at 50°C) for C_{org} to remove carbonates (Cauwet et al., 1990). The precision for C_{org} and total carbon (C_t) analyses was ±2%. Concentrations are expressed as the weight percent of dry sediment.

3.3. Modeling Pore Water Hg Profiles

The porewater Hg^{II}_{inorg} or MMHg profiles result from transport processes and reactions that release these species to or remove them from the aqueous phase. Assuming steady-state and neglecting advective fluxes, the distribution of porewater Hg can be described by the following one-dimensional mass balance equation (Berg et al., 1998; Boudreau, 1997). This equation accounts for the effect of molecular diffusion (D_S), bioturbation (D_B), and irrigation (α as the irrigation coefficient).

$$\left(\frac{\delta C}{\delta t}\right)_x = \frac{\delta}{\delta x}\left(\phi(D_S + D_B)\frac{\delta C}{\delta x}\right) + \phi\alpha(C_0 - C) + R_{net} = 0$$

where x is the depth coordinate, C is the dissolved concentration of mercury species in porewater, C_0 is the concentration in the water overlaying the sediments, ϕ is the porosity of the sediment, D_S is the sediment diffusivity, α is the irrigation coefficient and R_{net} is the rate of production ($R_{net} > 0$) or consumption ($R_{net} < 0$).

We calculated the sediment diffusivity (D_S) by considering the sediment porosity ϕ and the diffusion coefficients of Hg species in water (D_W). The latter is corrected for temperature using the Stokes-Einstein equation.

$$D_S = \phi^2 \times D_W$$

The diffusion coefficients D_W in water at 25°C for different Hg species (Hg^{II}_{inorg} and MMHg) are 9.5×10^{-6} $cm^2\ s^{-1}$ (Gill et al., 1999) and 1.2×10^{-5} $cm^2\ s^{-1}$ (Hammerschmidt & Fitzgerald, 2004), respectively. The porosity of the RR Prodelta is taken from a previous study by Cathalot et al. (2010).

Bioturbation and bioirrigation in these empirical calculations are constrained by adjusting coefficients D_B and α to biological field survey data, that is, the abundance and composition of the benthic macrofauna community. A previous assessment of the spatiotemporal changes in benthic macrofauna composition of the study site revealed the dominance of polychetes (>80% of the total abundance) but also significant temporal variations at the Rhone Prodelta mouth (Bonifácio et al., 2014). Minimal abundance and species richness were observed in the spring period (April–May) while the reduced water levels in the summer, that is, drier months, support the establishment of a more mature benthic macrofauna community. We collected sediment samples and deployed the Peepers during a period of spring-to-summer transition (May–July), but there was significant river discharge in June 2011 (Figure S3 in Supporting Information S1). Therefore, we assumed that such conditions would not be favorable for the establishment of benthic macrofauna and thus bioirrigation and bioturbation might not be significant. Accordingly, we assumed these processes negligible in the reaction rate calculations ($D_B = 0$ and $\alpha = 0$). Therefore, the equation is reduced to:

$$\left(\frac{\delta C}{\delta t}\right)_x = \frac{\delta}{\delta x}\left(\phi D_S \frac{\delta C}{\delta x}\right) + R_{net} = 0$$

This one-dimensional mass conservation equation was numerically solved for the net rate of production or consumption of Hg species per unit volume R_{net} using the computer code PROFILE (Berg et al., 1998).

4. Results and Discussion

4.1. Redox Chemistry of the Prodelta Sediments

The early diagenesis of OM in the Rhône prodelta sediments has already been examined and even scrutinized by multiple studies (Cathalot, 2008; Cathalot et al., 2010, 2013; Goineau et al., 2012; Lansard et al., 2008; Pastor et al., 2011a, 2011b, 2018; Rassmann et al., 2016, 2020). In brief, oxygen is rapidly consumed within the first cm below SWI (e.g., Lansard et al., 2008), followed by nitrate, Mn-Fe oxides, and sulfate utilization, pursuant to the established model for OM degradation in marine sediments (e.g., Froelich et al., 1979). According to Cathalot (2008) and Rassmann et al. (2016), 90% of the degraded OM in the sediment is anaerobic via sulfate reduction. These processes were at work at Sta. ME during our experiment as illustrated by the results we describe in the section below.

The C_{org} content in the solid phase varied between 1.8% and 2.9% with a decreasing tendency with depth (Figure 2a). The dissolved oxygen concentration at the SWI always remained higher than 200 µM during the Peepers deployment period (Fuchs, 2019), and consequently, the most superficial layer of sediments (~1 cm below the SWI) has remained oxic. The Fe^{II} and Mn^{II} concentration distributions (Peepers B and C) disclose the oxic conditions in the epibenthic waters and, at least, down to ~1 cm in pore waters (Figures 3e and 3f). Concurrently, the distribution of SO_4^{2-} in the pore waters showed that sulfate reduction started below 13 cm, and SO_4^{2-} concentrations regularly decreased with increasing depth (Figure 3a), suggesting the formation of sulfides (not measured). Interestingly, the dissolved Ca profiles mirrored the sulfate distribution (Figure 3b). This observation is coherent with previous studies in the proximal prodelta (Rassmann et al., 2016), which showed that $CaCO_3$ precipitation occurs due to the increase of porewater saturation state according to the process described by Mucci et al. (2000).

The distributions of nutrients (Figures 3c and 3d) and other redox-sensitive elements (Figures 3e and 3f) showed concentration peaks between SWI and the depth of sulfate reduction initiation. However, the occurrence of

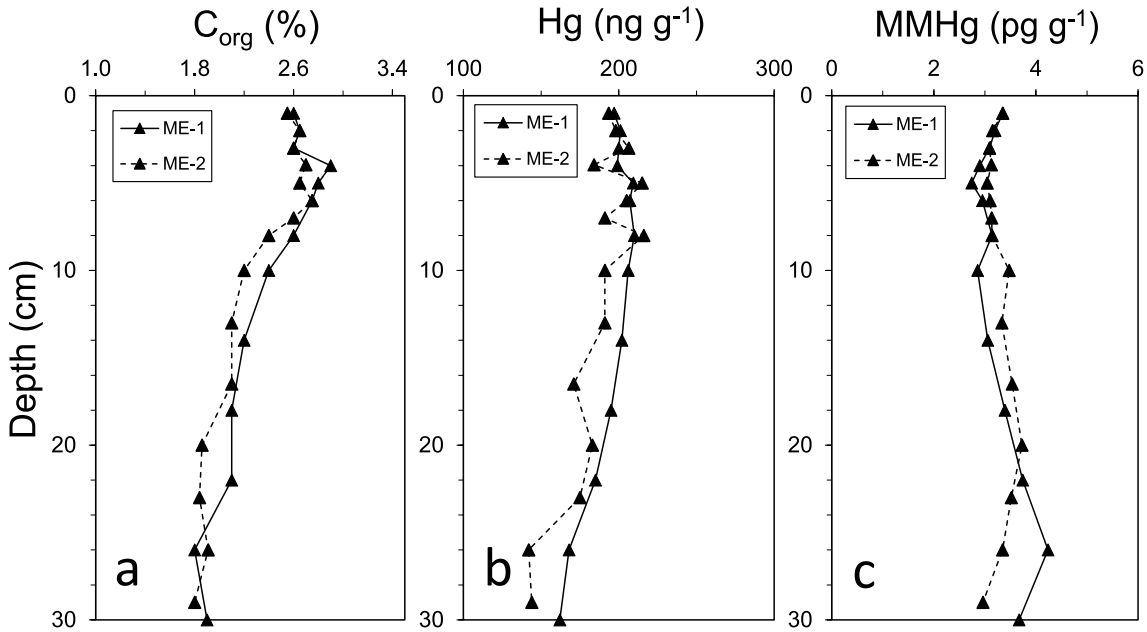

Figure 2. (a) Organic carbon (C_{org}), (b) total mercury (Hg), and (c) monomethyl Hg (MMHg) in the solid phase of the sediment cores (ME-1 and ME-2) collected at Sta. ME.

double-peak distributions of several redox species is observed further down in the sediment. Such a phenomenon has already been described for Fe^{II} in sediments collected in the same area (Pastor et al., 2018; Rassmann et al., 2020). There, close to the Rhône mouth, the sediments rapidly accumulate with maximal deposition of riverine particles during high water of the RR, as shown by short-live radionuclides (^{7}Be, ^{234}Th) distributions (Wu et al., 2018). Episodic inputs of sediments generate multiple-peak distributions for several redox-sensitive elements in the suboxic zone because of pulsed supplies of electron acceptors. According to Pastor et al. (2018), the episodic pulsed inputs of sediments supply the proximal prodelta sediments with enough oxides to inhibit any accumulation of free sulfide in the porewater. A former SWI may have been buried by the sudden and massive input of fresh sedimentary OM, such as those already reported in the proximal part of the prodelta (Cathalot et al., 2010; Marion et al., 2010) and in other Mediterranean coastal sediments (Dang et al., 2014a, 2014b) provoking transient early diagenetic processes. Alternatively, this feature may have been created by a sediment resuspension event. Both processes are accustomed in the study area. According to the continuous records at Sta. ME, the magnitude of the discharge change was insufficient to induce a massive input of riverine sediments (Figure S3a in Supporting Information S1) whereas an increase in turbidity, up to 4-fold the background level, started to develop in the third week of May 2011 to return to the background after a few days (Fuchs, 2019). The peak of turbidity recorded at Sta. ME (Figure S3b in Supporting Information S1) precedes the maximum in RR flow level suggesting that the resuspension of sediments is more probably induced by waves. These deposition conditions may constitute the reason why multipeak distributions of some redox-sensitive elements were observed since this delay is too short for allowing steady-states to be installed for all the reactions involved.

4.2. Mercury Distributions

4.2.1. Solid Phase

Total Hg and MMHg distributions in the solid phase of the two sediment cores collected at Sta. ME are shown in Figure 2b. Mercury concentrations ranged from 142 to 216 ng g^{-1}; these values are relatively low for sediments accumulated within the second half of the twentieth century in the Rhône prodelta (Cossa et al., 2024), where Hg concentrations have reached up to 700 ng g^{-1} (Augier et al., 1980) and confirm the decrease of the Hg contamination of the RR inputs observed in the last decades (Cossa et al., 2018; Poulier et al., 2019). There was little change in Hg concentrations over the 30 cm of the cores, only a slight decrease with depth below a homogeneous layer of 10 cm thick (Figure 2b). This limited Hg variability was expected since the pulsive character and the

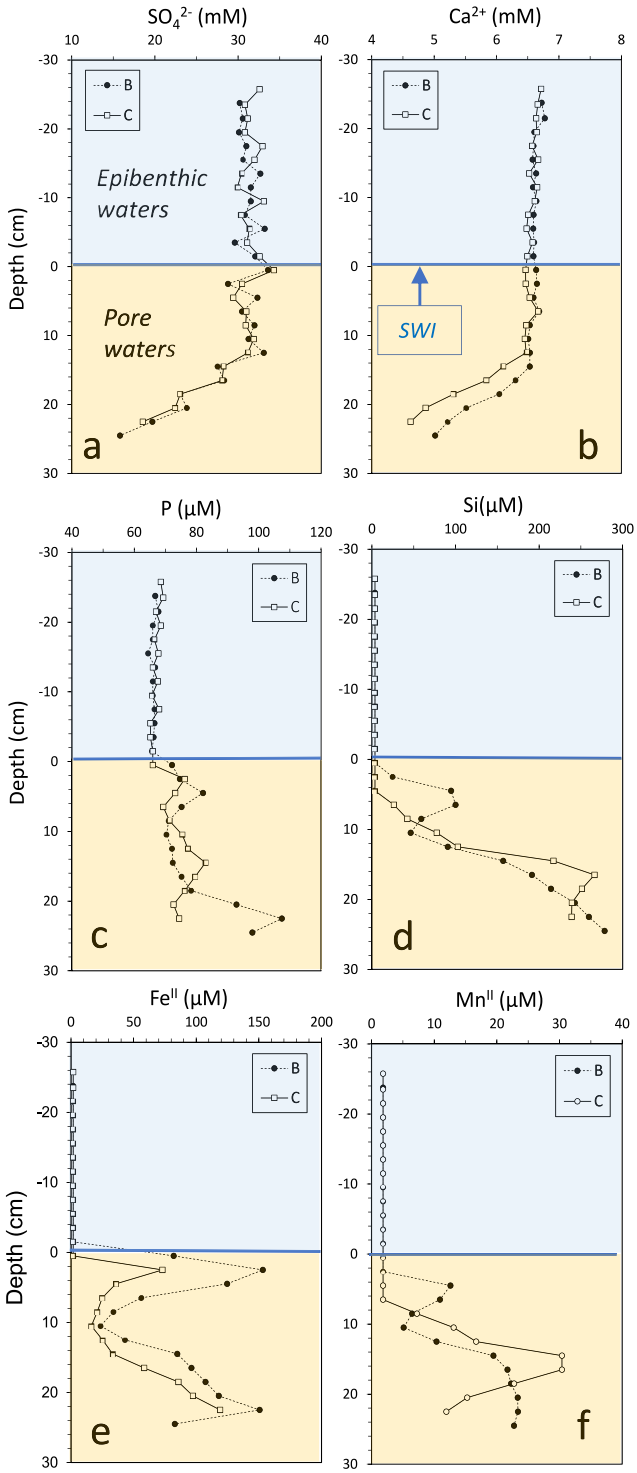

Figure 3. Distribution of major and redox elements in pore waters of Peepers A, B, C, and D implanted at Sta. ME. (a) SO_4^{2-}; (b) Ca^{2+}; (c) P; (d) $Si(OH)_4$; (c) Fe; (f) Mn. The blue line indicates the sediment-water interface (sediment-water interfaces).

age (≤one-year) of the deposited sediments (SR: 30–50 cm a^{-1}, Charmasson et al., 1998). However, the downward decrease in Hg concentrations was covariant with C_{org} profiles ($R = 0.75$, $n = 28$, $p < 0.01$). This suggests that part of particulate Hg could be mobilized in pore waters during OM degradation. Besides, the distribution of MMHg, which represents approximately 0.3%–0.5% of total Hg, does not show any depth trend (Figure 2c).

4.2.2. Dissolved Phase

The main feature of dissolved Hg concentration profiles was the contrast between Hg^{II}_{inorg} versus MMHg. Indeed, Hg^{II}_{inorg} concentrations were high (up to 0.580 nM) in the epibenthic water but remained much lower in pore waters (Figures 4a and 4b). Conversely, MMHg concentrations were significant in porewaters (up to 0.005 nM) but negligible in epibenthic waters (Figures 4c and 4d).

The Hg^{II}_{inorg} concentrations in the epibenthic zone were 10–200 times higher than the concentrations of the overlying water column (~0.003 nM according to Figure 3a in Cossa et al., 2018) depending on the Peeper. In Peepers A and B, the Hg^{II}_{inorg} profiles were typified by a double peak with the first 20 cm above the SWI (Figure 4a), whereas, in Peepers C and D, the Hg^{II}_{inorg} maxima were centered closer to the SWI (Figure 4b). This first-time revealed epibenthic pattern suggests the Hg^{II}_{inorg} mobilization within a water layer in the immediate vicinity above the SWI, akin to the nepheloid layer. The nepheloid layers are known in coastal areas for their intensive OM mineralization and are characterized by the presence of strong chemical gradients, including nutrients released by OM degradation (e.g., Gadel et al., 1993; Knoery et al., 2019; Pakhomova et al., 2018; Ransom et al., 1998; Yahel et al., 2008). The presence of double peaks in Peepers A and B is likely the result of the SWI changes that occurred at the beginning of the Peepers' deployment period. In the sediment pore waters, Hg^{II}_{inorg} concentrations (<0.004–0.082 nM depending on the Peeper) were comparable to those of western Atlantic estuarine and shelf sediments (Balcom et al., 2015; Hollweg et al., 2010); the mobility of these species in pore waters are addressed in the next Section 4.3.

The MMHg concentrations in epibenthic waters varied from 0.1 to 0.4 pM, a similar range to that of the GoL coastal water column (Cossa et al., 2017). This indicates that the MMHg distribution in the water column of coastal waters of the GoL is not noticeably affected by the proximity of the SWI. In pore waters, MMHg concentrations were 10 times less than those reported for contaminated estuarine sediments (Covelli et al., 2011; Gill et al., 1999; Gobeil & Cossa, 1993; Merritt & Amirbahman, 2008), but in the same order of magnitude as values for pore waters of Atlantic continental shelf sediments (Hollweg et al., 2010). The highest MMHg levels (4–5 pM) were located below 13 cm in Peepers A, B, and D (Figures 4c and 4d), corresponding to the sulfate reduction zone (Figure 3a). Furthermore, MMHg and SO_4^{2-} were inversely correlated ($R = -0.47$, $p < 0.01$). Additional MMHg peaks were systematically observed between 3 and 10 cm, a zone also characterized by P, Mn^{II}, and Fe^{II} peaks (Figure 3), tracers of redox reactions reminiscent of the model of OM diagenesis. Note that Pearson's correlation coefficients between MMHg and these redox tracers were statistically significant, with values of 0.78, 0.66, and 0.46 ($p < 0.01$), respectively. This may have resulted from the MMHg mobilization from solid sediment caused by OM degradation and/or from the methylation of Hg^{II}_{inorg} mitigated by sulfate-reducing and ferri-reducing microorganisms, according to the current paradigms (e.g., Compeau & Bartha, 1985; Flemming et al., 2006; Gilmour et al., 2011).

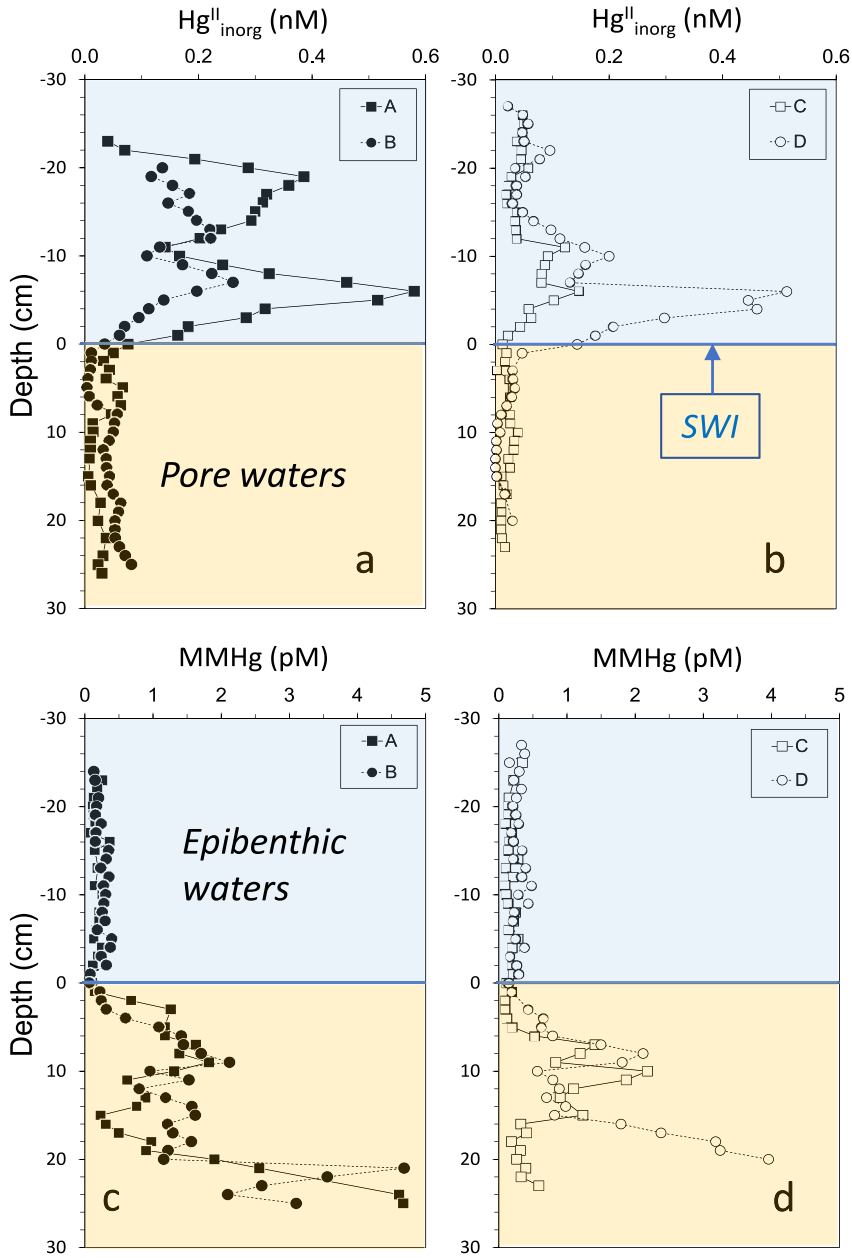

Figure 4. Distribution of Hg species in pore water of Peepers A, B, C, and D implanted at Sta. ME. (a and b) Hg^{II}_{inorg}; (c and d) MMHg. The blue line indicates the sediment-water interface (sediment-water interfaces).

This later interpretation is corroborated by the results of a Principal Component Analysis (Figure S4 in Supporting Information S1). MMHg correlates with F1 (R = 0.66 and 0.72, respectively) which is driven positively by Fe^{II} (R = 0.79) and negatively by SO_4^{2-} (R = −0.81). This strongly suggests that Hg^{II} methylation is driven by ferri- and sulfate-reducing bacteria.

4.3. Mercury and Methylmercury Dynamics

4.3.1. Verification of the Steady-State Assumption

One key step to validate the applicability of the one-dimensional mass conservation equation and the code PROFILE is to ensure that stationary sedimentary conditions occurred during the peepers' implementation. This could be performed following the procedure used by Couture et al. (2010), which consists of a direct comparison

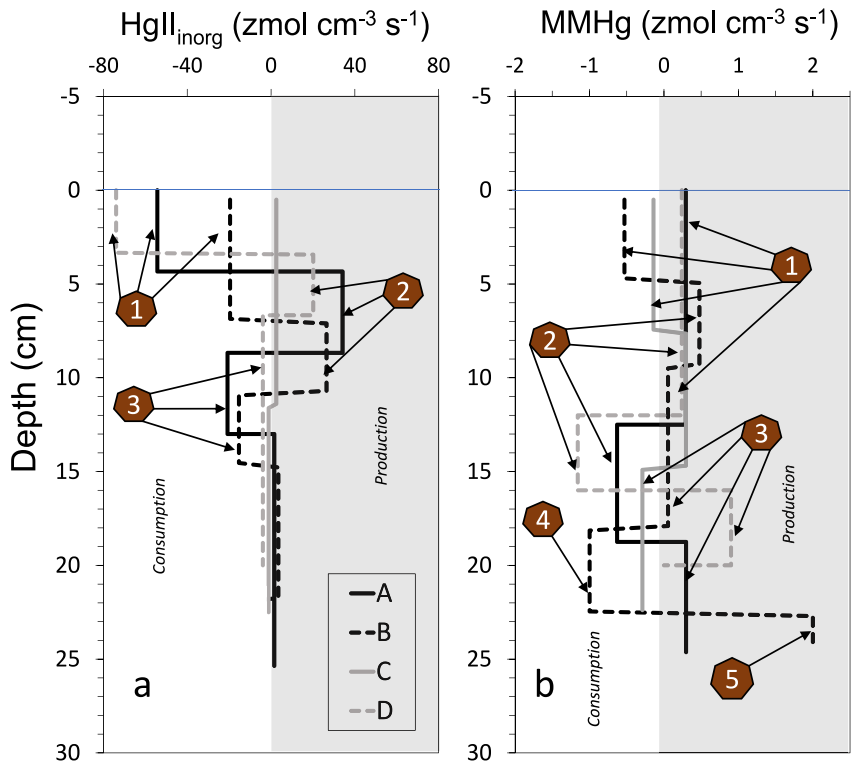

Figure 5. Modeled profiles for Hg^{II}_{inorg} and MMHg distributions at Sta. ME. Net (+) production and (−) consumption rates are presented in the gray and white areas, respectively. zmol is 10^{-21} mol. The blue line indicates the sediment-water interfaces. The numbers in brown polygons refer to zones defined in Table S1 in Supporting Information S1, with differences depending on the Peeper.

of the reaction time (τ_R, in seconds) to the duration of seasonal changes in the sedimentary system (τ_S). The former is calculated based on the average concentrations of Hg species within a layer of sediments of depth x (C_x) and the reaction rate for the corresponding sediment layer determined by PROFILE ($\tau_R = C/R_{net}$). The duration of the sedimentary condition stability was assumed to be 50 days ($\tau_S \sim 4.3 \times 10^6$ s), which is the duration of the June–July period during which no sediment resuspension was observed, see Figure S3b in Supporting Information S1. We then calculated the ratios τ_S/τ_R to evaluate if the reactions involving Hg were fast enough (i.e., high values of τ_S/τ_R relative to 1) to assume a steady-state treatment which can lead to reasonable estimates of consumption or production rates R_{net}. The calculated τ_S/τ_R ratios (Table S1 in Supporting Information S1) ranged between 1.7 and 10.3 for Hg^{II}_{inorg} (except for Peeper C), and between 1.0 and 4.8 for MMHg (except in Peeper B in zone 3, Figure 5b, for which the calculated production is very low, $R_{net} = 0.05$ zmol cm^{-3} s^{-1}, e.i., $0.05 \cdot 10^{-21}$ mol cm^{-3} s^{-1}). We can conclude that, with the two exceptions quoted above, the reaction times are smaller than the time scale of the sedimentary change and that the assumption of a quasi-steady state is reasonable.

In addition, there is also the need to compare the relative importance of biogeochemical reactions involving Hg against the physical diffusion process. The Damköhler numbers (DaD) are commonly used to relate the chemical reaction timescale (τ_R) to the transport phenomena rate (τ_D). The rate τ_D is characteristic of diffusion and can be calculated as $\tau_D = L^2/D_S$, based on the thickness L of a consumption/production zone and the sediment diffusivity D_S (see Section 3.3.). DaD is equal to τ_D/τ_R; values of DaD larger than 1 imply that the biogeochemical transformation of Hg species outpaces diffusion. In all the Peepers (except in zone 3 of Peeper B), DaD values are higher than 1, varying from 1.0 to 9.8 for Hg^{II}_{inorg}, and from 1.0 to 5.2 for MMHg (Table S1 in Supporting Information S1), which indicates that reaction dominates over diffusion. Thus, modeling the pore water profiles of the three Peepers to infer reaction rates is a reasonable approach (Couture et al., 2010).

The optimization of the number of zones to fit the vertical profiles using the code PROFILE was based on the F statistics (p-values for the comparison of different fits and an assessment of goodness-of-fit, i.e., the sum of squared deviations and correlation coefficients R^2). Overall, the p-values of our fits were better than 0.01 and

the sums of squared deviations were three to four orders of magnitude lower than the averaged concentrations. The profiles modeled for the Hg species and the measurements were in good agreement with R^2 of 0.91–0.99 for $Hg^{II}_{inorg,}$ and 0.85–0.95 for MMHg; the modeled production (+) and consumption (−) zones were generally consistent between the various profiles. Figure 5 consists of the piecewise constant functions representing the net Hg and MMHg production or consumption rates following the measured values showing the PROFILE model fitting.

4.3.2. Inorganic Hg

The R_{net} values for Hg^{II}_{inorg} (from −74 to +34 zmol cm^{-3} s^{-1}) were consistent with the rate levels reported by Merritt & Amirbahman (2007) for the contaminated Penobscot estuarine sediments (−14 to +52 zmol cm^{-3} s^{-1}). Except for Peeper C (for which the steady-state condition is not realized: $S/tR < 1$, Table S1 in Supporting Information S1), the Hg^{II}_{inorg} production/consumption profiles exhibit three successive zones (4-to-6 cm thick) below the SWI constrained within the first half of the pore water column (<15 cm). Below these zones, the R_{net} was close to zero (Figure 5a). From the SWI downward, one can observe: a consumption zone, then a production zone followed by another consumption layer. The upper consumption zone (zone 1 in Figure 5a) includes the oxic layer and the Fe^{II} gradients suggesting the oxy(hydr)oxides precipitation within the first cm below the SWI (Figure 3). The lower consumption zone (zone 3 in Figure 5a) of Hg^{II}_{inorg} corresponds to the Fe^{II} minima, suggesting some Fe compound (FeS) precipitation just below the constant SO^{2-}_4 layer. This hypothesis is supported by the observation of enrichment of FeS minerals in the same area of the proximal Rhône prodelta sediments (Rassmann et al., 2020).

In between the two Hg consumption zones, the layer of Hg^{II}_{inorg} production (zone 2, Figure 5a) includes the Si, P, Fe, and Mn maxima (Figure 3), suggesting the Hg^{II}_{inorg} is solubilized during the OM degradation or dissolution of oxy(hydr)oxides or even their consortium. This interpretation is supported by the fact that Fe is produced in the first 2 cm and consumed around 10 cm below the SWI. It is well established, from experimental and field measurements or modeling, that solid minerals (e.g., Fe-oxy(hydr)oxides and Fe-sulfides) adsorb various Hg species in environmental conditions (Andren & Harriss, 1975; Huerta-Diaz & Morse, 1999; Jeong et al., 2007; Kim et al., 2004; Tiffreau et al., 1995). In addition, observations in lake sediments and their modeling highlight Hg adsorption onto authigenic Fe oxy(hydr)oxides in oxic sediments and on Fe sulfide phases and sulfidized OM under anoxic conditions (Feyte et al., 2012; Skyllberg, 2008). The presence of these minerals has been documented in the RR prodelta sediments (e.g., Pastor et al., 2018; Rassmann et al., 2020), and similar Hg phase change has already been shown to occur in the "Fe reduction" zone of marine coastal sediments (Oliveri et al., 2016); the recent identification of Hg-S-Fe nanoparticles in anaerobic environments may provide a mechanism for these observations (Ji et al., 2023).

4.3.3. Methylmercury

The calculated rates of MMHg consumption and production rates ranged from −1.2 to +2.0 zmol cm^{-3} which is more restricted than the range calculated in the Penobscot Estuary sediments (ranging from −42 to +49 zmol cm^{-3} s^{-1}), all values calculated with the same technique (Feyte et al., 2012; Merritt & Amirbahman, 2008). In the first half of the sedimentary column below the SWI (in the first 12 cm below the SWI), R_{net} were very low for Peepers A, C, and D (−0.14 to 0.24 zmol cm^{-3} s^{-1}, zone 1 in Figure 5b); such close to zero reaction rates are mainly related to diffusion. In these cases, with a sharp gradient close to the SWI, the numerical averaging may improperly influence the identification of the mechanism supporting MMHg data interpretation (Merritt & Amirbahman, 2009). Peeper B exhibited a negative value for Peepers B (−0.53 zmol cm^{-3} s^{-1} in zone 1in Figure 5b) which indicates a net MMHg consumption in pore water near the SWI, which precludes any significant MMHg flux in the overlying waters. Mechanisms for this loss include adsorption onto oxy(hydr)oxides and/or MMHg demethylation.

In the second part of the sedimentary column (i.e., roughly below 12 cm), consumption zones are also identified as zone 2 for Peeper A and D, and zone 4 for Peeper B, which overhang production zones (zones 3 and 5, Figure 5b). The production zones below 13 cm coincide with the sulfate reduction zone and suggest Hg methylation by sulfate-reducing bacteria as noted above. The MMHg consumption just below the SWI may result from the adsorption of MMHg on OM associated with Fe-oxy(hydr)oxides in the authigenic material (Feyte et al., 2010). Alternatively, it may result from net demethylation controlled by numerous types of microorganisms in both aerobic and anoxic environments either by reductive or oxidative processes (Barkay et al., 2011; Mason, 2012). We can test the hypothesis that the negative R_{net} is entirely due to MMHg demethylation by computing the demethylation constant (k_d) from the present observations, according to Feyte et al. (2012) approach:

$$R_{net} = R_{ads} + R_m + R_d$$

where R_{ads} represents the rate of MMHg removal by adsorption, and R_m and R_d the rates of methylation and demethylation, respectively. According to the hypothesis that adsorption and methylation are neglectable in the surficial consumption zone, it follows that the demethylation rate can be derived from the R_{net}:

$$R_{net} \approx R_d = -\phi\, k_d\, [MMHg]_{av}$$

where k_d (d^{-1}) is the apparent first-order constant and the subscript "av" is the MMHg average values over the first cm below the SWI (see Feyte et al., 2012 for details). Applied to Peepers B and C MMHg profiles within the 4 cm below the interface, we calculated a mean k_d of 0.23 $days^{-1}$, a value in the range of experimental-derived lake sediment values, that is, ~0.5 $days^{-1}$ for sites without identified Hg sources (Helmrich et al., 2022) and an order of magnitude lower than the range North–west Atlantic estuarine sediments (3.6–15.8 $days^{-1}$ according to Heyes et al., 2006).

Still under the first 12 cm below the SWI, when examining Peepers B and C for which redox profiles are available, it appears that the corresponding MMHg consumption (R_{net}) is unrelated to Fe chemistry (Figure 3e), but to the intensity of bacterial activity illustrated by the dissolved phosphorus profiles (Figure 3c). This suggests that (a) sorption processes onto iron sulfide, is not the primary operating mechanism in the MMHg removing processes from pore waters and (b) that microbiologically mediated reaction, namely demethylation (methylation), might control the consumption (production) of this species in the sediments. If we apply the approach developed for k_d calculation to the estimate of the k_m, using the data of the Peepers A, B, and D in the deep zone of net MMHg production and inorganic Hg ($[Hg]_{av}$) instead of $[MMHg]_{av}$, we arrive with k_m of 0.001–0.006 $days^{-1}$, in the low range of the values obtained by Heyes et al. (2006) in estuarine sediments (0.002–0.044 $days^{-1}$) and an order of magnitude lower than the "reasonable range" (0.04 ± 0.03 $days^{-1}$) for wetland sediments (Helmrich et al., 2022). This difference may result from the lower availability of Hg^{II}_{inorg} for methylating bacteria in natural environments compared to the added inorganic Hg isotopes used in the laboratory or ex-situ experiments. The results of these calculations strongly suggest that MMHg distribution in pore water is controlled by microbiological in situ reactions.

4.4. The Sedimentary Outflux of Hg^{II} and MMHg in Epibenthic Waters

As underlined in the introduction of the present paper, there is large uncertainty about the importance of coastal sediments as a source of Hg species for the overlying water column. Several studies in coastal and estuarine sediment pore waters have concluded to the diffusing of MMHg across the SWI and consequently the possible MMHg-enrichment of the overlying water column (e.g., Bothner et al., 1980; Hammerschmidt & Fitzgerald, 2006; Hammerschmidt et al., 2004; Hollweg et al., 2010). Most of these studies have been carried out using diffusive models and poorly defined MMHg gradients across the SWI and were contradicted by more recent results (e.g., Sunderland et al., 2010). Besides, benthic chambers have suggested that Hg methylation in the sediments was a source of MMHg for the water column through diffusion (e.g., Covelli et al., 1999; Monperrus et al., 2007). However, the MMHg enrichment observed in the benthic chambers may as well be the result of Hg methylation in the chamber itself. More recently, interface samplers, of Peepers' type (Rigaud et al., 2013) or recently conceived ones, such as SUSANE (Knoery et al., 2019), have allowed the assessment of the distribution of chemicals in the epibenthic layer allowing the assessment high-resolution gradients in the vicinity of the SWI and offer more convincing conclusions. In the present study, the MMHg profiles across the pore and the epibenthic waters (Figures 4c and 4d) do not allow us to identify the existence of a diffusive MMHg transport across the SWI (Figure S5 in Supporting Information S1). More likely, the more probable potential efflux of MMHg from the Rhône prodelta sediments to the underlying water column should be through sediment resuspension; this process has been estimated for the entire GoL sediments to deliver 3 kg of MMHg each year to the water column (Cossa et al., 2017); in these conditions, assuming a surface area of 10 km^2 for the proximal part of the RR prodelta, the MMHg delivered from the sediments can be estimated around 2 g a^{-1}.

On the other hand, the Hg^{II}_{inorg} enrichment in the dissolved phase (Figures 4a and 4b) in the epibenthic water column sampled with the Peepers (i.e., the 30-cm thick water column above the SWI) suggests a Hg mobilization during the particulate OM degradation into the nepheloid layer whose extension in the entire Rhône prodelta has been described for more than 40 years (Aloïsi et al., 1982; Buscail et al., 1990). The dissolution and degradation of the particulate OM in the aerobic conditions of this area favor the mobilization of Hg^{II}_{inorg} at the expense of MMHg formation, which is favored by suboxic or anoxic conditions. From the present Hg profiles in the

epibenthic zone of the prodelta, the Hg^{II}_{inorg} enrichment within 30 cm above the SWI averaging 0.25 nM represents 80 times the concentration of the rest of the water column. This is a significant amount since it constitutes almost 10 times the Hg content of the entire water column. Assuming an area of 10 km^2 for the prodelta area this enrichment represents an additional ∼150 g of Hg^{II}_{inorg}. Based on the C_{org} mineralization (16.7 g m^{-2} a^{-1}) occurring in the benthic nepheloid layer for the entire GoL by Buscail et al. (1990), and a Hg:C_{org} mass ratio of $\sim 0.8 \cdot 10^{-7}$, we can calculate a Hg^{II}_{inorg} mobilization of ∼20 kg a^{-1}, which a comparable amount to that provided annually by the RR to the Mediterranean in the form of dissolved Hg species (∼26 kg a^{-1} according to Cossa et al., 2018). The fate of the Hg^{II}_{inorg} mobilized in the epibenthic waters is uncertain. On the one hand, it can be potentially available for further methylation, on the other it can be re-adsorbed on flocculating material and be ultimately incorporated into surface sediments. At least, the fate of the Hg^{II}_{inorg} mobilized in the epibenthic waters and its interaction with underlying sediments deserves to be studied.

5. Conclusions

Our results show for the first time that Hg^{II}_{inorg} is mobilized in a significant amount in the epibenthic layer just close above the SWI in a coastal marine environment. As the Hg concentrations peak 200 times the concentration of the overlying water column, this process is of major importance in reintroducing dissolved Hg^{II}_{inorg} into the water column. These Hg species may become available for methylation by microorganisms, bioaccumulation by autotrophic organisms, and further biomagnification in higher trophic-level animals. On the other hand, our results suggest that the diffusion of MMHg from the sediment, even where sulfate-reduction is an important pathway for OM degradation, is a negligible source for underlying coastal waters. The MMHg produced in the pore waters may be delivered into the water column but mainly via sediment resuspension on the occasion of storms or high waters in the river. Alternatively, this molecule may be incorporated into coastal food webs through the benthic fauna.

In summary, we show that the epibenthic proximal zone of the Rhône prodelta is a place of intense mobilization of Hg^{II}_{inorg} associated with OM mineralization and that the diffusion of MMHg from sediment pore waters, where sulfate reduction is a major process for OM degradation, is a minor way for the mobilization of Hg in the water column. It would be of great interest to test whether the observations made in the sediments and nepheloid layer of the Rhône prodelta could be extrapolated to other ocean margins and how the abyssal sediments behave relative to the Hg post-depositional mobility. We can speculate that the very low SR of the deep ocean should not favor Hg accumulation during OM maturation, which occurs mainly in the water column and the deep nepheloids, favoring Hg mobilization before burial. In practice, for the management purpose of contaminated environments, the estimation of the amount of Hg^{II}_{inorg} bioavailable for methylation and the magnitude of MMHg formation and mobility should be included in risk evaluation.

Conflict of Interest

The authors declare no conflicts of interest relevant to this study.

Data Availability Statement

Map of the study area (Figure 1) was made using PowerPoint (Microsoft). Figures 2–5 were made using Excel (Microsoft). All the data presented in this study have been included in the Supporting Information (Tables S1 and S2 in Supporting Information S1) and have been deposited in the facilities of PANGAEA (Data Publisher for Earth & Environmental Science): https://doi.org/10.1594/PANGAEA.964517.

Acknowledgments
This paper has benefited from data from the MINERHO project and has been funded by the project Mistrals/MERMEX-Rivers, the French state program "Investissement d'avenir" run by the National Research Agency (AMORAD). Many thanks are also due to C. Ravel and E. Emery for the scuba diving sampling operations and to Anne Tabard-Fougère for her assistance in the statistical treatment. Raoul-Marie Couture is especially thanked for his helpful comments on an early version of the manuscript.

References

Abi-Ghanem, C., Nakhlé, K., Khalaf, G., & Cossa, D. (2011). Mercury distribution and methylmercury mobility in the sediments of three sites on the Lebanese Coast, Eastern Mediterranean. *Archives of Environmental Contamination and Toxicology*, *60*(3), 394–405. https://doi.org/10.1007/s00244-010-9555-9

Adams, D. D. (1994). Sediment pore water sampling. Chap 7. In D. A. Mudroch & S. D. MacKnight (Eds.), *Handbook of techniques for aquatic sediments sampling* (pp. 171–201). Lewis Publisher Inc. CRC Press.

Aller, J. Y., & Aller, R. C. (2004). Physical disturbance creates bacterial dominance of benthic biological communities in tropical deltaic environments of the Gulf of Papua. *Continental Shelf Research*, *24*(19), 2395–2416. https://doi.org/10.1016/j.csr.2004.07.015

Aloïsi, J. C., Cambon, P., Carbonne, J., Cauwet, G., Millot, C., Monaco, A., & Pauc, H. (1982). Origine et rôle du néphéloïde profond dans le transfert des particules en milieu marin. Application au Golfe du Lion. *Oceanologica Acta*, *5*(4), 481–491. https://archimer.ifremer.fr/doc/00121/23188/

AMAP/UN Environment. (2019). *Technical background Report for the global mercury assessment 2018*. Arctic Monitoring and Assessment Programme, Oslo, Norway/UN Environment Programme, Chemicals and Health Branch, Geneva, Switzerland. viii + 426 pp including E-Annexes. Retrieved from https://www.amap.no/documents/doc/technical-background-report-for-the-global-mercury-assessment-2018/1815

Andren, A. W., & Harriss, R. C. (1975). Observations on the association between mercury and organic matter dissolved in natural waters. *Geochimica et Cosmochimica Acta*, *39*(9), 1253–1257. https://doi.org/10.1016/0016-7037(75)90132-5

Antonelli, C. (2002). *Flux sédimentaires et morphogénèse récente dans le chenal du Rhône aval*. Thèse de doctorat. Université Aix-Marseille I, France. 279p. https://www.theses.fr/2002AIX10058

Augier, H., Gilles, G., & Romanda, G. (1980). Première estimation de la pollution mercurielle du littoral méditerranéen français. Prog. Wat. Tech. In *Mediterranean coastal pollution. Proceedings of a conference held in Palma, Mallorca, Sept. 1979. S.H. Jenkins editor* (Vol. 12(1), pp. 97–108). IAWPR/Pergamon Press. https://doi.org/10.1016/B978-0-08-026058-7.50012-1

Balcom, P. H., Schartup, A. T., Mason, R. P., & Chen, C. Y. (2015). Sources of water column methylmercury across multiple estuaries in the Northeast U.S. *Marine Chemistry*, *177*, 721–730. https://doi.org/10.1016/j.marchem.2015.10.012

Barkay, T., Kroer, N., & Poulain, A. J. (2011). Some like it cold: Microbial transformations of mercury in polar regions. *Polar Research*, *30*(1), 15469. https://doi.org/10.3402/polar.v30i0.15469

Berg, P., Risgaard-Petersen, N., & Munkegade, N. (1998). Interpretation of measured concentration profiles in sediment pore water. *Limnology & Oceanography*, *43*(7), 1500–1510. https://doi.org/10.4319/lo.1998.43.7.1500

Berner, R. A. (1980). *Early diagenesis: A theoretical approach*. Princeton University Press.

Berner, R. A. (1989). Biogeochemical cycles of carbon and sulfur and their effect on atmospheric oxygen over phanerozoic time. *Global and Planetary Change*, *75*(1–2), 97–122. https://doi.org/10.1016/0921-8181(89)90018-0

Boening, D. W. (2000). Ecological effects, transport, and fate of mercury: A general review. *Chemosphere*, *40*(12), 1335–1351. https://doi.org/10.1016/s0045-6535(99)00283-0

Bonifácio, P., Bourgeois, S., Labrune, C., Amouroux, J. M., Escoubeyrou, K., Buscail, R., et al. (2014). Spatiotemporal changes in surface sediment characteristics and benthic macrofauna composition off the Rhône River in relation to its hydrological regime. *Estuarine, Coastal and Shelf Science*, *151*, 196–209. https://doi.org/10.1016/j.ecss.2014.10.011

Bothner, M. H., Jahnke, R. A., Peterson, M. L., & Carpenter, R. (1980). Rate of mercury loss from contaminated estuarine sediments. *Geochimica et Cosmochimica Acta*, *44*(2), 273–285. https://doi.org/10.1016/0016-7037(80)90137-4

Boudreau, B. P. (1997). *Diagenetic models and their implementation: Modelling transport and reactions in aquatic sediments* (p. 398pp). Springer. https://doi.org/10.1007/97S-3-642-60421-S

Bowie, A. R., & Lohan, M. C. (2008). Analysis of iron in seawater. Chap. 12. In O. Wurl (Ed.), *Practical guidelines for the analysis of iron in seawater* (p. 408p). Taylor & Francis. https://doi.org/10.1201/9781420073072

Bravo, A. G., & Cosio, C. (2019). Biotic formation of methylmercury: A bio–physico–chemical conundrum. *Limnology & Oceanography*, *65*(5), 1–18. https://doi.org/10.1002/lno.11366

Burdige, D. J. (2005). Burial of terrestrial organic matter in marine sediments: A re-assessment. *Global Biogeochemical Cycles*, *19*(4). https://doi.org/10.1029/2004GB002368

Buscail, R., Pocklington, R., Daumas, R., & Guidi, L. (1990). Fluxes and budget of organic matter in the benthic boundary layer over the northwestern Mediterranean margin. *Continental Shelf Research*, *10*(9–11), 1089–1122. https://doi.org/10.1016/0278-4343(90)90076-X

Carignan, R., Rapin, F., & Tessier, A. (1985). Sediment porewater sampling analysis: A comparison of techniques. *Geochimica et Cosmochimica Acta*, *49*(11), 2493–2497. https://doi.org/10.1016/0016-7037(85)90248-0

Cathalot, C. (2008). *Devenir et impact des apports fluviaux sur les marges continentales: Importance biogéochimique et environnementale du recyclage dans les sédiments du prodelta du Rhône*. Thèse de doctorat. Specialité Sciences de l'Environnement; Université P. et M. Curie (Paris 6, France). 194pp. Retrieved from https://theses.hal.science/tel-00813147

Cathalot, C., Rabouille, C., Pastor, L., Deflandre, B., Viollier, E., Buscail, R., et al. (2010). Temporal variability of carbon recycling in coastal sediments influenced by rivers: Assessing the impact of flood inputs in the Rhone River prodelta. *Biogeosciences*, *7*(3), 1187–1205. https://doi.org/10.5194/bg-7-1187-2010

Cathalot, C., Rabouille, C., Tisnérat-Laborde, N., Toussaint, F., Kerhervé, P., Buscail, R., et al. (2013). The fate of river organic carbon in coastal areas: A study in the Rhône River delta using multiple isotopic ($\delta^{13}C$, $\Delta^{14}C$) and organic tracers. *Geochimica et Cosmochimica Acta*, *118*, 33–55. https://doi.org/10.1016/j.gca.2013.05.001

Cauwet, G., Gadel, F., De Souza Sierra, M. M., Donard, O., & Ewald, M. (1990). Contribution of the Rhône River to organic inputs to the Northwestern Mediterranean Sea. *Continental Shelf Research*, *10*(9–11), 1025–1037. https://doi.org/10.1016/0278-4343(90)90073-U

Chakraborty, P., Sarkar, A., Vudamala, K., Naik, R., & Nath, B. N. (2015). Organic matter-a key factor in controlling mercury distribution in estuarine sediment. *Marine Chemistry*, *173*, 302–309. https://doi.org/10.1016/j.marchem.2014.10.005

Charmasson, S., Bouisset, P., Radakovitch, O., Pruchon, S. A., & Arnaud, M. (1998). Long-core profiles of Cs-137, Cs-134, Co-60, and Pb-210 in sediment near the Rhone River (Northwestern Mediterranean Sea). *Estuaries*, *21*(3), 367–378. https://doi.org/10.2307/1352836

Compeau, G., & Bartha, R. (1985). Sulfate-reducing bacteria: Principal methylators of mercury in anoxic estuarine sediments. *Applied and Environmental Microbiology*, *50*(2), 498–502. https://doi.org/10.1128/aem.50.2.498-502.1985

Cossa, D., Averty, B., & Pirrone, N. (2009). The origin of methylmercury in the open Mediterranean water column. *Limnology & Oceanography*, *54*(3), 837–844. https://doi.org/10.4319/lo.2009.54.3.0837

Cossa, D., Buscail, R., Dennielou, B., Radakovitch, O., Puig, P., Khripounoff, A., et al. (2024). Sources, transport, and accumulation of mercury in the northwestern Mediterranean margin sediments during the Industrial Era. *Progress in Oceanography*, *220*, 103186. https://doi.org/10.1016/j.pocean.2023.103186

Cossa, D., Durrieu de Madron, X., Schäfer, J., Guédron, S., Marusczak, N., Castelle, S., & Naudin, J.-J. (2018). Sources and exchanges of mercury in the waters of the Northwestern Mediterranean margin. *Progress in Oceanography*, *163*, 172–183. https://doi.org/10.1016/j.pocean.2017.05.002

Cossa, D., Durrieu de Madron, X., Schäfer, J., Lanceleur, L., Guédron, S., Buscail, R., et al. (2017). The open sea as the main source of methylmercury in the water column of the Gulf of Lions (Northwestern Mediterranean margin). *Geochimica et Cosmochimica Acta*, *199*, 212–231. https://doi.org/10.1016/j.gca.2016.11.037

Cossa, D., Garnier, C., Buscail, R., Elbaz-Poulichet, F., Mikac, N., Patel-Sorrentino, N., et al. (2014). A Michaelis-Menten type equation for describing methylmercury dependence on inorganic mercury in aquatic sediments. *Biogeochemistry*, *119*(1–3), 35–43. https://doi.org/10.1007/s10533-013-9924-3

Couture, R.-M., Gobeil, C., & Tessier, A. (2010). Arsenic, iron and sulfur co-diagenesis in lake sediments. *Geochimica et Cosmochimica Acta*, *74*(4), 1238–1255. https://doi.org/10.1016/j.gca.2009.11.028

Covelli, S., Emili, A., Acquavita, A., Koron, N., & Faganeli, J. (2011). Benthic biogeochemical cycling of mercury in two contaminated northern Adriatic coastal lagoons. *Continental Shelf Research*, *31*(16), 1777–1789. https://doi.org/10.1016/j.csr.2011.08.005

Covelli, S., Faganeli, J., Horvat, M., & Brambati, A. (1999). Porewater distribution and benthic flux measurements of mercury and methylmercury in the Gulf of Trieste (Northern Adriatic Sea). *Estuarine, Coastal and Shelf Science*, *48*(4), 415–428. https://doi.org/10.1006/ecss.1999.0466

Dang, D. H., Lenoble, V., Durrieu, G., Mullot, J.-U., Mounier, S., & Garnier, C. (2014b). Sedimentary dynamics of coastal organic matter: An assessment of the porewater size/reactivity model by spectroscopic techniques. *Estuarine, Coastal and Shelf Science*, *151*, 100–111. https://doi.org/10.1016/j.ecss.2014.10.002

Dang, D. H., Tessier, E., Lenoble, V., Durrieu, G., Omanović, D., Mullot, J.-U., et al. (2014a). Key parameters controlling arsenic dynamics in coastal sediments: An analytical and modeling approach. *Marine Chemistry*, *161*, 34–46. https://doi.org/10.1016/j.marchem.2014.02.005

Feyte, S., Gobeil, C., Tessier, A., & Cossa, D. (2012). Mercury dynamics in lake sediments. *Geochimica et Cosmochimica Acta*, *82*, 92–112. https://doi.org/10.1016/j.gca.2011.02.007

Feyte, S., Tessier, A., Gobeil, C., & Cossa, D. (2010). *In situ* adsorption of mercury, methylmercury and other elements by iron oxyhydroxides and organic matter in lake sediments. *Applied Geochemistry*, *25*(7), 984–995. https://doi.org/10.1016/j.gca.2010.04.005

Fitzgerald, W. F., Lamborg, C. H., & Hammerschmidt, C. R. (2007). Marine biogeochemical cycling of mercury. *Chemical Review*, *107*(2), 641–662. https://doi.org/10.1021/cr050353m

Flemming, E. J., Marck, E. E., Green, P. G., & Nelson, D. C. (2006). Mercury methylation from unexpected sources: Molybdate-inhibited freshwater sediments and an iron-reducing bacterium. *Applied and Environmental Microbiology*, *72*(1), 457–464. https://doi.org/10.1128/AEM.72.1.457-464.2006

Frieling, J., Mather, T. A., März, C., Jenkyns, H. C., Hennekam, R., Reichart, G.-J., et al. (2023). Effects of redox variability and early diagenesis on marine sedimentary Hg records. *Geochimica et Cosmologica Acta*, *351*, 78–95. https://doi.org/10.1016/j.gca.2023.04.015

Froelich, P. N., Klinkhammer, G. P., Bender, M. L., Luedtke, N. A., Heath, G. R., Cullen, D., et al. (1979). Early oxidation of organic matter in pelagic sediments of the eastern equatorial Atlantic: Suboxic diagenesis. *Geochimica et Cosmochimica Acta*, *43*(7), 1075–1090. https://doi.org/10.1016/0016-7037(79)90095-4

Fuchs, R. (2019). Qualification des données Mesurho 2009–2018. *Rapport Ifremer/ Ler-Pac N° 19-09*, 45p. https://doi.org/10.13155/62695

Gadel, F., Charrière, B., & Serve, L. (1993). Chemical characterization of suspended particulate organic matter by pyrolysis-gas chromatography coupled with mass spectrometry and high performance liquid chromatography in the bottom nepheloid layer of the Rhône Delta. *Estuarine, Coastal and Shelf Science*, *37*(3), 221–236. https://doi.org/10.1006/ecss.1993.1053

Gangloff, A., Verney, R., Doxartan, D., Ody, A., & Estournel, C. (2017). Investigating Rhône River plume (Gulf of Lions, France) dynamics using metrics analysis from the MERIS 300m Ocean Color archive (2002–2012). *Continental Shelf Research*, *144*, 98–111. https://doi.org/10.1016/j.csr.2017.06.024

Gill, G. A., Bloom, N. S., Cappellino, S., Driscoll, C. T., Dobbs, C., McShea, L., et al. (1999). Sediment–Water fluxes of mercury in Lavaca Bay, Texas. *Environmental Science & Technology*, *33*(5), 663–669. https://doi.org/10.1021/es980380c

Gilmour, C. C., Elias, D. A., Kucken, A. M., Brown, S. D., Palumbo, A. V., Schadt, C. W., & Wall, J. D. (2011). Sulfate-reducing bacterium *Desulfovibrio desulfuricans* ND132 as a model for understanding bacterial mercury methylation. *Applied and Environmental Microbiology*, *77*(12), 938–3951. https://doi.org/10.1128/AEM.02993-10

Gobeil, C., & Cossa, D. (1993). Mercury in sediments and sediment pore water in the Laurentian Trough. *Canadian Journal of Fisheries and Aquatic Sciences*, *50*(8), 1794–1800. https://doi.org/10.1139/f93-201

Goineau, A., Fontanier, C., Jorissen, F., Buscail, R., Kerhervé, P., Cathalot, C., et al. (2012). Temporal variability of live (stained) benthic foraminiferal faunas in a river-dominated shelf – Faunal response to rapid changes of the river influence (Rhône prodelta, NW Mediterranean). *Biogeosciences*, *9*(4), 1367–1388. https://doi.org/10.5194/bg-9-1367-2012

Gosnell, K. J., & Mason, R. P. (2015). Mercury and methylmercury incidence and bioaccumulation in plankton from the central Pacific Ocean. *Marine Chemistry*, *177*(5), 772–780. https://doi.org/10.1016/j.marchem.2015.07.005

Gworek, B., Bemowska-Kalabun, O., Kijenska, M., & Wrosek-Jakubowska, J. (2016). Mercury in marine and oceanic waters – A review. *Water, Air, and Soil Pollution*, *227*(10), 371. https://doi.org/10.1007/s11270-016-3060-3

Hammerschmidt, C. R., & Fitzgerald, W. F. (2004). Geochemical controls on the production and distribution of methylmercury in near-shore marine sediments. *Environmental Science & Technology*, *38*(5), 1487–1495. https://doi.org/10.1021/es034528

Hammerschmidt, C. R., & Fitzgerald, W. F. (2006). Bioaccumulation and trophic transfer of methylmercury in Long Island Sound. *Archives of Environmental Contamination and Toxicology*, *51*(3), 416–424. https://doi.org/10.1007/s00244-005-0265-7

Hammerschmidt, C. R., Lamborg, C. H., Balcom, P. H., & Visscher, P. T. (2004). Biogeochemistry of methylmercury in sediments of Long Island Sound. *Marine Chemistry*, *90*(1–4), 31–52. https://doi.org/10.1016/j.marchem.2004.02.024

Helmrich, S., Vlassopoulos, D., Alpers, C. N., & O'Day, P. A. (2022). Critical review of mercury methylation and methylmercury demethylation rate constants in aquatic sediments for biogeochemical modeling. *Critical Reviews in Environmental Science and Technology*, *52*(24), 4353–4378. https://doi.org/10.1080/10643389.2021.2013073

Hesslein, R. H. (1976). An in situ sampler for close interval pore water studies. *Limnology & Oceanography*, *21*(6), 912–914. https://doi.org/10.4319/lo.1976.21.6.0912

Heyes, A., Mason, R. P., Kim, E.-H., & Sunderland, E. (2006). Mercury methylation in estuaries: Insights from using measuring rates using mercury isotopes. *Marine Chemistry*, *102*(1–2), 134–147. https://doi.org/10.1016/j.marchem.2005.09.018

Hollweg, T. A., Gilmour, C. C., & Mason, R. P. (2010). Mercury and methylmercury cycling in sediments of the mid-Atlantic continental shelf and slope. *Limnology & Oceanography*, *55*(6), 2703–2722. https://doi.org/10.4319/lo.2010.55.6.2703

Hong, Y., Dan, N. P., Kim, E., Choi, H.-J., & Han, S. (2014). Application of diffusive gel-type probes for assessing redox zonation and mercury methylation in the Mekong Delta sediment. *Environmental Science: Processes & Impacts*, *16*(7), 1799–1808. https://doi.org/10.1039/C3EM00728F

Huerta-Diaz, M., & Morse, J. W. (1999). Pyritization of trace metals in anoxic marine sediments. *Geochimica et Cosmochimica Acta*, *56*(7), 268l–2702l. https://doi.org/10.1016/0016-7037(92)90353-K

Jeong, H. Y., Klaue, B., Blum, J., & Hayes, K. F. (2007). Sorption of mercuric ion by Synthetic Nanocrystalline Mackinawite (FeS). *Environmental Science & Technology*, *41*(22), 7699–7705. https://doi.org/10.1021/es070289l

Ji, Y., Gao, S., Si, R., Zhang, Z., Tian, L., Guan, W., et al. (2023). Structural incorporation of iron influences biomethylation potential of mercury sulfide. *Geochimica et Cosmochimica Acta*, *349*, 115–125. https://doi.org/10.1016/j.gca.2023.03.035

Kim, C. S., Rytuba, J. J., & Brown, G. E., Jr. (2004). EXAFS study of mercury(II) sorption to Fe- and Al-(hydr)oxides I. Effects of pH. *Journal of Colloid and Interface Science*, *271*(1), 1–15. https://doi.org/10.1016/s0021-9797(03)00330-8

Knoery, J., Cossa, D., Thomas, B., Germain, G., & Rigaud, S. (2019). Susane, a device for sampling chemical gradients in the benthic water column. *Limnology and Oceanography: Methods*, *17*(6), 331–342. https://doi.org/10.1002/lom3.10317

Kraepiel, A. M. L., Keller, K., Chin, H. B., Malcolm, E. G., & Morel, F. M. M. (2003). Sources and variations of mercury in Tuna. *Environmental Science & Technology*, *37*(24), 5551–5558. https://doi.org/10.1021/es0340679

Lansard, B., Rabouille, C., Denis, L., & Genz, C. (2008). In situ oxygen uptake rates by coastal sediments under the influence of the Rhône River (NW Mediterranean Sea). *Continental Shelf Research*, *28*(12), 1501–1510. https://doi.org/10.1016/j.csr.2007.10.010

Lansard, B., Rabouille, C., Denis, L., & Grenz, C. (2009). Benthic remineralization at the land-ocean interface: A case study of the Rhone River (NW Mediterranean Sea). *Estuarine, Coastal and Shelf Science*, *81*(4), 544–554. https://doi.org/10.1016/j.ecss.2008.11.025

Lavoie, R. A., Jardine, T. D., Chumchal, M. M., Kidd, K. A., & Campbell, L. M. (2013). Biomagnification of mercury in aquatic food webs: A worldwide meta-analysis. *Environmental Science & Technology*, *47*(23), 13385–13394. https://doi.org/10.1021/es403103t

Lee, C. S., & Fisher, N. S. (2017). Bioaccumulation of methylmercury in a marine diatom and the influence of dissolved organic matter. *Marine Chemistry*, *197*, 70–79. https://doi.org/10.1016/j.marchem.2017.09.005

Marion, C., Dufois, F., Arnaud, M., & Vella, C. (2010). In situ record of sedimentary processes near the Rhone River mouth during winter events (Gulf of Lions, Mediterranean Sea). *Continental Shelf Research*, *30*(9), 1095–1107. https://doi.org/10.1016/j.csr.2010.02.015

Marvin-DiPasquale, M., & Agee, J. L. (2003). Microbial mercury cycling in sediments of the San Francisco Bay-Delta. *Estuaries*, *26*(6), 1517–1528. https://doi.org/10.1007/bf02803660

Mason, R. P. (2012). The methylation of metals and metalloids in aquatic systems (Chap. 11). In A. Dricu (Ed.), *Methylation—from DNA, RNA, and histones to diseases and treatment* (pp. 271–301). INTECH Open Science. Retrieved from https://www.intechopen.com/chapters/38950

Mason, R. P., Bloom, N., Cappellino, S., Gill, G., Benoit, J., & Dobbs, C. (1998). Investigation of porewater sampling methods for mercury and methylmercury. *Environmental Science & Technology*, *32*(24), 4031–4040. https://doi.org/10.1021/es980377t

Mason, R. P., Reinfelder, J. R., & Morel, F. M. M. (1996). The uptake, toxicity, and trophic transfer of mercury in a coastal diatom. *Environmental Science & Technology*, *30*(6), 1835–1845. https://doi.org/10.1021/es950373d

MasonChoi, R. P. A. L., Fitzgerald, W. F., Hammerschmidt, C. R., Lamborg, C. H., Soerensen, A. L., & Sunderland, E. M. (2012). Mercury biogeochemical cycling in the ocean and policy implications. *Environmental Research*, *119*, 101–117. https://doi.org/10.1016/j.envres.2012.03.013

Mergler, D. (2021). Ecosystem approaches to mercury and human health: A way toward the future. *Ambio*, *50*(3), 527–531. https://doi.org/10.1007/s13280-020-01455-0

Merritt, K. A., & Amirbahman, A. (2007). Mercury dynamics in sulfide-rich sediments: Geochemical influence on contaminants mobilization within the Penobscot River estuary, Maine, USA. *Geochimica et Cosmochimica Acta*, *71*(4), 929–941. https://doi.org/10.1016/j.gca.2006.10.012

Merritt, K. A., & Amirbahman, A. (2008). Methylmercury cycling in estuarine sediment pore waters (Penobscot River estuary, Maine, USA). *Limnology & Oceanography*, *53*(3), 1064–1075. https://doi.org/10.4319/lo.2008.53.3.1064

Merritt, K. A., & Amirbahman, A. (2009). Mercury methylation dynamics in estuarine and coastal environments – A critical review. *Earth-Science Reviews*, *96*(1–2), 54–66. https://doi.org/10.1016/j.earscirev.2009.06.002

Miralles, J., Radakovitch, O., & Aloisi, J.-C. (2005). Pb-210 sedimentation rates from the Northwestern Mediterranean margin. *Marine Geology*, *216*(3), 155–167. https://doi.org/10.1016/j.margeo.2005.02.020

Monperrus, M., Tessier, E., Point, D., Vidimova, K., Amouroux, D., Guyoneaud, R., et al. (2007). The biogeochemistry of mercury at the sediment-water interface in the Thau lagoon. 2. Evaluation of mercury methylation potential in both surface sediment and the water column. *Estuarine, Coastal and Shelf Science*, *72*(3), 485–496. https://doi.org/10.1016/j.ecss.2006.11.014

Mucci, A., Sundby, B., Gehlen, M., Arakaki, T., Zhong, S., & Silverberg, N. (2000). The fate of carbon in continental shelf sediments of eastern Canada: A case study. *Deep-Sea Research II*, *47*(3–4), 733–760. https://doi.org/10.1016/S0967-0645(99)00124-1

Muresan, B., Cossa, D., Jézéquel, D., Prévot, F., & Kerbellec, S. (2007). The biogeochemistry of mercury at the sediment-water interface in the Thau lagoon. 1. Partition and speciation. *Estuarine, Coastal and Shelf Science*, *72*(3), 472–484. https://doi.org/10.1016/j.ecss.2006.11.015

Oliveri, E., Manta, D. S., Bonsignore, M., Cappello, S., Tranchida, G., Bagnato, E., et al. (2016). Mobility of mercury in contaminated marine sediments: Biogeochemical pathway. *Marine Chemistry*, *186*, 1–10. https://doi.org/10.1016/j.marchem.2016.07.002

Pakhomova, S., Yakushev, E., Protsenko, E., Rigaud, S., Cossa, D., Knoery, J., et al. (2018). Modeling the influence of eutrophication and redox conditions on mercury cycling at the sediment-water interface in the Berre Lagoon. *Frontiers in Marine Science*, *5*(291), 1–5. https://doi.org/10.3389/fmars.2018.00291

Pastor, L., Cathalot, C., Deflandre, B., Viollier, E., Soetaert, K., Meysman, F. J. R., et al. (2011a). Modeling biogeochemical processes in sediments from the Rhone River prodelta area (NW Mediterranean Sea). *Biogeosciences*, *8*(5), 1351–1366. https://doi.org/10.5194/bg-8-1351-2011

Pastor, L., Deflandre, B., Viollier, E., Cathalot, C., Metzger, E., Rabouille, C., et al. (2011b). Influence of the organic matter composition on benthic oxygen demand in the Rhone River prodelta (NW Mediterranean Sea). *Continental Shelf Research*, *31*(9), 1008–1019. https://doi.org/10.1016/j.csr.2011.03.007

Pastor, L., Rabouille, C., Metzger, E., Thibault de Chanvalon, A., Viollier, E., & Deflandre, B. (2018). Transient early diagenetic processes in Rhône prodelta sediments revealed in contrasting flood events. *Continental Shelf Research*, *166*, 65–76. https://doi.org/10.1016/j.csr.2018.07.005

Pont, D., Simonnet, J. P., & Walter, A. V. (2002). Medium-term changes in suspended sediment delivery to the ocean: Consequences of catchment heterogeneity and river management (Rhone River, France). *Estuarine, Coastal and Shelf Science*, *54*(1), 1–18. https://doi.org/10.1006/ecss.2001.0829

Poulier, G., Launay, M., Le Bescond, C., Thollet, F., Coquery, M., & Lecoz, J. (2019). Combining flux monitoring and data reconstruction to establish annual budgets of suspended particulate matter, mercury and PCB in the Rhône River from Lake Geneva to the Mediterranean Sea. *Science of the Total Environment*, *658*, 457–473. https://doi.org/10.1016/j.scitotenv.2018.12.075

Ransom, B., Shea, K. F., Burkett, P. J., Bennett, R. H., & Baerwald, R. (1998). Comparison of pelagic and nepheloid layer marine snow: Implications for carbon cycling. *Marine Geology*, *150*(1–4), 39–50. https://doi.org/10.1016/s0025-3227(98)00052-8

Rassmann, J., Eitel, E. M., Lansard, B., Cathalot, C., Brandily, C., Taillefert, M., & Rabouille, C. (2020). Benthic alkalinity and dissolved inorganic carbon fluxes in the Rhône River prodelta generated by decoupled aerobic and anaerobic processes. *Biogeosciences*, *17*(1), 13–33. https://doi.org/10.5194/bg-17-13-2020

Rassmann, J., Lansard, B., Pozzato, L., & Rabouille, C. (2016). Carbonate chemistry in sediment porewaters of the Rhône River delta driven by early diagenesis (northwestern Mediterranean). *Biogeosciences*, *13*(18), 5379–5394. https://doi.org/10.5194/bg-13-5379-2016

Rigaud, S., Radakovitch, O., Couture, R. M., Deflandre, B., Cossa, D., Garnier, C., & Garnier, J.-M. (2013). Mobility and fluxes of trace elements and nutrients at the sediment-water interface of a lagoon under contrasting water column oxygenation conditions. *Applied Geochemistry*, *31*, 35–51. https://doi.org/10.1016/j.apgeochem.2012.12.003

Roussiez, V., Ludwig, W., Monaco, A., Probst, J.-L., Bouloubassi, I., Buscail, R., & Saragoni, G. (2006). Sources and sinks of sediment-bound contaminants in the gulf of lions (NW Mediterranean sea): A multi-tracer approach. *Continental Shelf Research*, *26*(16), 1843–1857. https://doi.org/10.1016/J.CSR.2006.04.010

Sanei, H., Outridge, P. M., Dallimore, A., & Hamilton, P. B. (2012). Mercury-organic matter relationships in pre-pollution sediments of thermokarst lakes from the Mackenzie River Delta, Canada: The role of depositional environment. *Biogeochemistry*, *107*(1–3), 149–164. https://doi.org/10.1007/s10533-010-9543-1

Sempéré, R., Charriere, B., van Wambeke, F., & Cauwet, G. (2000). Carbon inputs of the Rhone River to the Mediterranean Sea: Biogeochemical implications. *Global Biogeochemical Cycles*, *14*(2), 669–681. https://doi.org/10.1029/1999GB900069

Skyllberg, U. (2008). Competition among thiols and inorganic sulfides and polysulfides for Hg and MeHg in wetland soils and sediments under suboxic conditions: Illumination of controversies and implications for MeHg net production. *Journal of Geophysical Research*, *113*(G2), G00C03. https://doi.org/10.1029/2008JG000745

Stoichev, T., Rodriguez Martin-Doimeadios, R. C., Tessier, E., Amouroux, D., & Donard, O. F. X. (2004). Improvement of analytical performances for mercury speciation by on-line derivatization, cryofocussing, and atomic fluorescence spectrometry. *Talanta*, *62*(2), 433–438. https://doi.org/10.1016/j.talanta.2003.08.006

Sunderland, E. M., Dalziel, J., Heyes, A., Branfireun, B. A., Krabbenhoft, D. P., & Gobas, F. A. P. C. (2010). Response of a macrotidal estuary to changes in anthropogenic mercury loading between 1850 and 2000. *Environment Science & Technology*, *44*(5), 1698–1704. https://doi.org/10.1021/es9032524

Sunderland, E. M., & Mason, R. P. (2007). Human impacts on open ocean mercury concentrations. *Global Biogeochemical Cycles*, *21*(4), GB 4022. https://doi.org/10.1029/2006GB002876

Tesán-Onrubia, J.-A., Heimbürger-Boavida, L.-E., Dufour, A., Harmelin-Vivien, H., García-Arévalo, I., Knoery, J., et al. (2023). Bioconcentration, bioaccumulation and biomagnification of mercury in plankton of the Mediterranean Sea. *Marine Pollution Bulletin*, *194*, 115439. Part B. https://doi.org/10.1016/j.marpolbul.2023.115439

Tesi, T., Miserocchi, S., Goni, M. A., & Langone, L. (2007). Source, transport, and fate of terrestrial organic carbon on the western Mediterranean Sea, Gulf of Lions, France. *Marine Chemistry*, *105*(1–2), 101–117. https://doi.org/10.1016/j.marchem.2007.01.005

Tiffreau, C., Lützenkirchen, J., & Behra, P. (1995). Modeling the adsorption of mercury(II) on (Hydr)oxides: I. Amorphous iron oxide and α-Quartz. *Journal of Colloid and Interface Science*, *172*(1), 82–93. https://doi.org/10.1006/jcis.1995.1228

Ulses, C., Estournel, C., Durrieu de Madron, X., & Palanques, A. (2008). Suspended sediment transport in the Gulf of Lions (NW Mediterranean): Impact of extreme storms and floods. *Continental Shelf Research*, *28*(15), 2048–2070. https://doi.org/10.1016/j.csr.2008.01.015

Wu, J., Rabouille, C., Charmasson, S., Reyss, J.-L., & Cagnat, X. (2018). Constraining the origin of recently deposited particles using natural radionuclides 7Be and 234Thex in deltaic sediments. *Continental Shelf Research*, *165*, 106–119. https://doi.org/10.1016/j.csr.2018.06.010

Yahel, G., Yahel, R., Katz, T., Lazar, B., Herut, B., & Tunnicliffe, V. (2008). Fish activity: A major mechanism for sediment resuspension and organic matter remineralization in coastal marine sediments. *Marine Ecology Progress Series*, *372*, 195–209. https://doi.org/10.3354/meps07688

Zebracki, M., Eyrolle-Boyer, F., Evrard, O., Claval, D., Mourier, B., Gairoard, S., et al. (2015). Tracing the origin of suspended sediment in a large Mediterranean river by combining continuous river monitoring and measurement of artificial and natural radionuclides. *Science of the Total Environment*, *502*, 22–132. https://doi.org/10.1016/j.scitotenv